

1 **Chemically-informed Analyses of Metabolomics Mass Spectrometry Data**

2 **with Qemistree**

3 Authors: Anupriya Tripathi^{1,2,3#}, Yoshiki Vázquez-Baeza^{4,5#}, Julia M. Gauglitz^{3,6}, Mingxun Wang³, Kai Dührkop⁷,
4 Mélissa Nothias-Esposito³, Deepa D. Acharya^{3,8}, Madeleine Ernst^{3,6,9}, Justin J.J. van der Hooft¹⁰, Qiyun Zhu²,
5 Daniel McDonald², Antonio Gonzalez², Jo Handelsman⁸, Markus Fleischhauer⁷, Marcus Ludwig⁷, Sebastian Böcker⁷,
6 Louis-Félix Nothias³, Rob Knight^{2,4,5,11}, Pieter C. Dorrestein^{3,5,6}

7

8 Author Affiliations:

9 ¹ Division of Biological Sciences, University of California San Diego.

10 ² Department of Pediatrics, University of California San Diego.

11 ³ Skaggs School of Pharmacy and Pharmaceutical Sciences, University of California San Diego

12 ⁴ Jacobs School of Engineering, University of California San Diego, La Jolla, California, USA.

13 ⁵ Center for Microbiome Innovation, University of California San Diego, La Jolla, California, USA.

14 ⁶ Collaborative Mass Spectrometry Innovation Center, Skaggs School of Pharmacy and Pharmaceutical Sciences,
15 University of California, San Diego, La Jolla, CA, USA.

16 ⁷ Chair for Bioinformatics, Friedrich-Schiller-University, Jena, Germany.

17 ⁸ Wisconsin Institute of Discovery, University of Wisconsin-Madison, Madison, Wisconsin, USA

18 ⁹ Section for Clinical Mass Spectrometry, Department of Congenital Disorders, Danish Center for Neonatal
19 Screening, Statens Serum Institut, Copenhagen, Denmark

20 ¹⁰ Bioinformatics Group, Plant Sciences Group, Wageningen University, Wageningen, The Netherlands.

21 ¹¹ Department of Computer Science and Engineering, University of California San Diego.

22 [#] Equal contribution.

23

24 Author contributions:

25 PCD, AT conceived the concept and managed the project.

26 AT and YVB developed the algorithm and wrote the code for Qemistree.

27 AT and YVB contributed equally to the work.

28 LFN, RK, PCD supervised method implementation.

29 KD, MW, JJvdH, ME, DM, and AG tested and provided suggestions on how to improve the method.

30 MW managed the deployment of Qemistree on GNPS.

31 AT and MW developed the GNPS-Qemistree Dashboard.

32 DA and AT wrote the documentation for the GNPS-Qemistree workflow.

33 YVB, QZ, and AT developed Qemistree-iTOL visualization.

34 LFN and MNE performed the mass-spectrometry for the evaluation dataset.

35 AT, YVB, and LFN analyzed and interpreted the evaluation data.

36 JMG performed mass spectrometry of the Global Foodomics samples.

37 AT, JMG analyzed and interpreted the Global Foodomics data.

38 KD, MF, ML, and SB supported the integration of SIRIUS, Zodiac, and CSI:FingerID.
39 PCD, AT, YVB, and RK wrote the manuscript.
40 LFN, JMG, MNE, JJvdH, ME, KD, QZ, DM, AG, JH, MF, ML, SB, and RK improved the manuscript.

41 Abstract

42 Untargeted mass spectrometry is employed to detect small molecules in complex biospecimens,
43 generating data that are difficult to interpret. We developed Qemistree, a data exploration
44 strategy based on hierarchical organization of molecular fingerprints predicted from
45 fragmentation spectra, represented in the context of sample metadata and chemical ontologies.
46 By expressing molecular relationships as a tree, we can apply ecological tools, designed around
47 the relatedness of DNA sequences, to study chemical composition.

48 Main

49 Molecular networking¹, introduced in 2012, was one of the first data organization approaches to
50 visualize the relationships between fragmentation spectra for similar molecules from tandem
51 mass spectrometry data in the context of metadata. It formed the basis for the web-based mass
52 spectrometry infrastructure, Global Natural Products Social Molecular Networking² (GNPS,
53 <https://gnps.ucsd.edu/>) which sees ~200,000 new accessions per month. Molecular networking is
54 used for a range of applications³ in drug discovery, environmental monitoring, medicine, and
55 agriculture. While molecular networking is useful for visualizing closely related molecular
56 families, the inference of chemical relationships at a dataset-wide level and in the context of
57 diverse metadata requires complementary representation strategies. To address this need, we
58 developed an approach that uses fragmentation trees⁴ and supervised machine learning⁵ to
59 calculate all pairwise chemical relationships and visualizes it in the context of sample metadata
60 and molecular annotations. We show that a chemical tree enables the application of various tree-
61 based tools, originally developed for analyzing DNA sequencing data⁶⁻⁹, for exploring mass-
62 spectrometry data.

63

64 We introduce Qemistree, pronounced *chemis-tree*, a software that constructs a chemical tree
65 from fragmentation spectra based on predicted molecular fingerprints¹⁰. Molecular fingerprints
66 are vectors where each position encodes a substructural property of the molecule. Recent
67 methods allow us to predict molecular fingerprints from tandem mass spectra¹¹⁻¹⁵. In Qemistree,

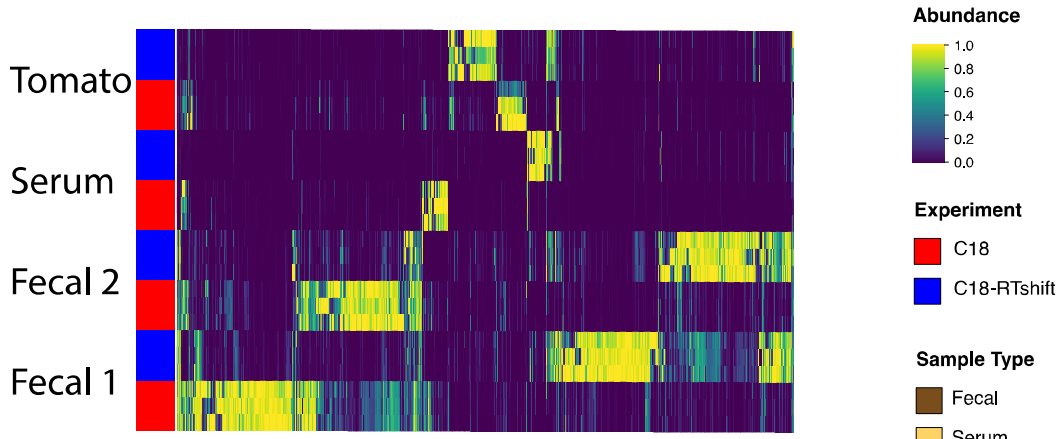
68 we use SIRIUS¹⁶ and CSI:FingerID¹³ to obtain predicted molecular fingerprints. The users first
69 perform feature detection^{17,18} to generate a list of observed ions, referred to as chemical features
70 henceforth, to be analyzed by Qemistree (Fig. S1). SIRIUS then determines the molecular
71 formula of each feature using the isotope and fragmentation patterns, and estimates the best
72 fragmentation tree explaining the fragmentation spectrum. Subsequently, CSI:FingerID operates
73 on the fragmentation trees using kernel support vector machines to predict molecular properties
74 (2936 properties; Table S1). We use these molecular fingerprints to calculate pairwise distances
75 between chemical features that are hierarchically clustered to generate a tree representing their
76 structural relationships. Although alternative approaches to hierarchically cluster features based
77 on cosine similarity of fragmentation spectra exist^{19–21}, we use molecular fingerprints as it allows
78 us to compare features based on a diverse range of structural properties predicted by
79 CSI:FingerID. Additionally, as CSI:FingerID was shown to perform well for automatic *in silico*
80 structural annotation²², we leverage it to search molecular structural databases to provide
81 complementary insights into structures when no match is obtained against spectral libraries.
82 Subsequently, we use ClassyFire²³ to assign a 5-level chemical taxonomy (kingdom, superclass,
83 class, subclass, and direct parent) to all molecules annotated via spectral library matching and *in*
84 *silico* prediction.

85
86 Phylogenetic tools such as iTOL²⁴ can be used to visualize Qemistree trees interactively in the
87 context of sample information and feature annotations for easy data exploration. The outputs of
88 Qemistree can also be plugged into other workflows in QIIME 2²⁵ (many of which were
89 originally developed for microbiome sequence analysis) or in R, Python etc. for system-wide
90 metabolomic data analyses^{6,7,9,26}. Qemistree is available to the microbiome community as a
91 QIIME 2 plugin (<https://github.com/biocore/q2-qemistree>) and the metabolomics community as
92 a workflow on GNPS² (<https://ccms-ucsd.github.io/GNPSDocumentation/qemistree/>). The
93 chemical tree from the GNPS workflow can be explored interactively (e.g.
94 <https://qemistree.ucsd.edu/>).

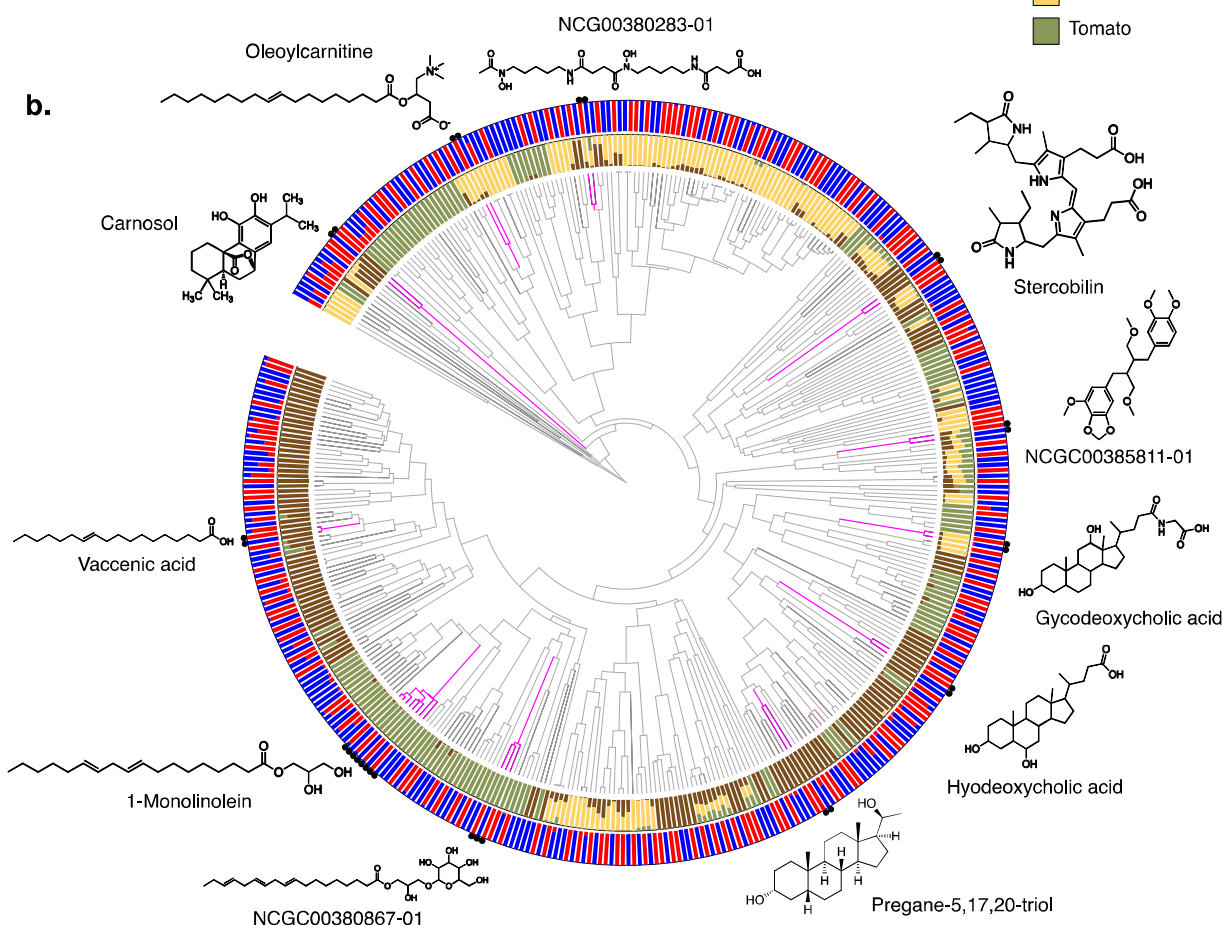
95
96 To verify that molecular fingerprint-based trees correctly capture the chemical relationships
97 between molecules, we generated an evaluation dataset with two human fecal samples, a tomato
98 seedling sample, and a human serum sample. Mixtures of these samples were prepared by

99 combining them in gradually increasing proportions to generate a set of diverse but related
100 metabolite profiles and untargeted tandem mass spectrometry was used to profile the chemical
101 composition of these samples. Mass-spectrometry was performed twice using different
102 chromatographic gradients causing a non-uniform retention time shift between the two runs. The
103 data processing of these two experiments leads to the same molecules being detected as different
104 chemical features in downstream analysis. In Figure 1a we highlight how these technical
105 variations make the same samples appear chemically disjointed.

a.



b.



106

107 **Figure 1: Chemistree mitigates aspects of technical artifacts by co-clustering structurally similar molecules**
 108 **across mass spectrometry runs. a)** Sample (y-axis) by molecule (x-axis) heatmap of 2 fecal samples, tomato
 109 seedling samples, and serum samples in the evaluation dataset grouped by chromatography conditions. **b)** A
 110 chemical tree based on predicted molecular fingerprints representing the structural relationships between compounds
 111 detected in the evaluation dataset. Outer ring shows the relative abundance of molecules stratified by mass
 112 spectrometry run; inner ring shows the same stratified by fecal, serum and tomato samples in the evaluation dataset.
 113 Structurally similar molecules detected as different chemical features due to shift in retention time across mass
 114 spectrometry runs are clustered together; we highlight some examples of these artificially duplicated features around
 115 the tree. All structures shown are spectral reference library matches obtained from feature-based molecular

116 networking¹⁷ in GNPS: (<https://gnps.ucsd.edu/ProteoSAFe/status.jsp?task=efda476c72724b29a91693a108fa5a9d>;
117 Metabolomics Standard Initiative (MSI) level 3 annotation)²⁷.
118

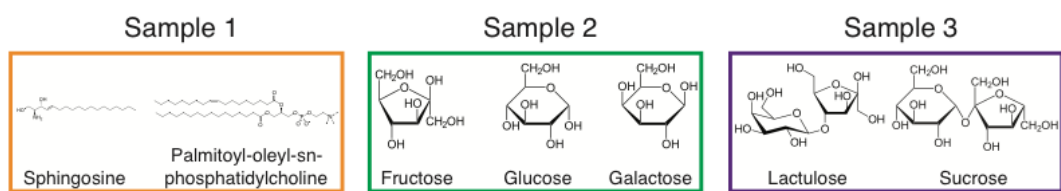
119 Using Qemistree, we map each of the spectra in the two chromatographic conditions (batches) to
120 a molecular fingerprint, and organize these in a tree structure (Fig. 1b). Because molecular
121 fingerprints are independent of retention time shifts, spectra are clustered based on their chemical
122 similarity. This tree structure can be decorated using sample type descriptions, chromatographic
123 conditions, and spectral library matches obtained from molecular networking in GNPS. Figure 1
124 shows that similar chemical features are detected exclusively in one of the two batches.
125 However, based on the molecular fingerprints, these chemical features were arranged as
126 neighboring tips in the tree regardless of the retention time shifts. This result shows how
127 Qemistree can reconcile and facilitate the comparison of datasets acquired on different
128 chromatographic gradients.

129

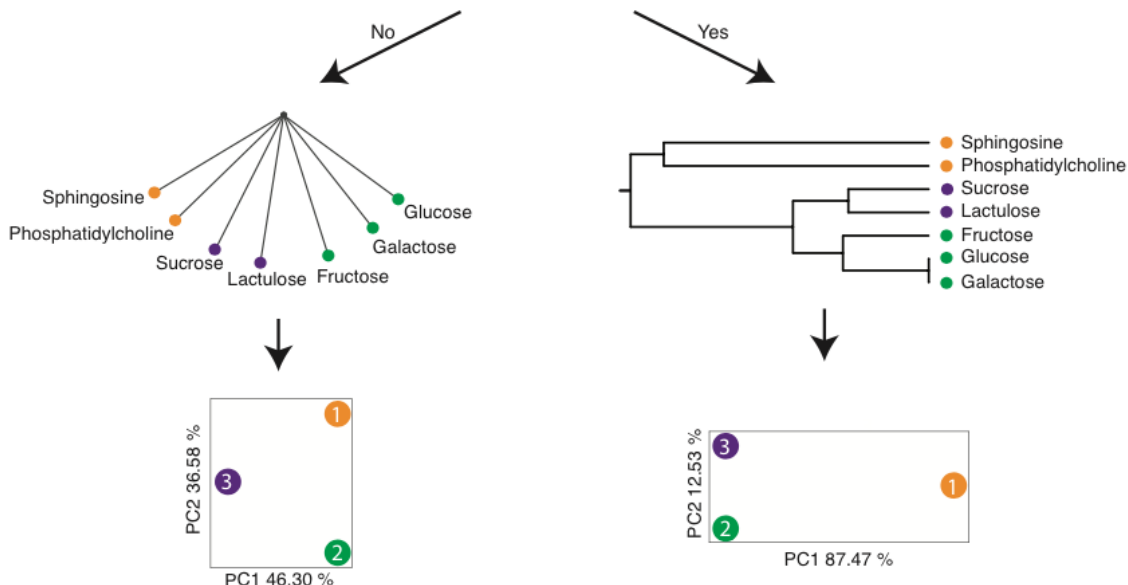
130 We demonstrate the use of a chemical hierarchy in performing chemically-informed
131 comparisons of metabolomics profiles. In standard metabolomic statistical analyses, each
132 molecule is assumed unrelated to the other molecules in the dataset. Some of the pitfalls of this
133 assumption are highlighted in Figure 2a. Consider a scenario where we want to compare samples
134 1-3. An analysis schema that does not account for the chemical relationships among the
135 molecules in these samples (Figure 2a, left), will assume that the sugars in samples 2 and 3 are as
136 chemically related to the lipids in sample 1 as they are to each other. This would lead to the naive
137 conclusion that samples 1 and 2, and samples 2 and 3 are equally distinct, yet they are not from a
138 chemical perspective. On the other hand, if we account for the fact that sugar molecules are more
139 chemically related to one another than they are to lipids, we can obtain a chemically-informed
140 sample-to-sample comparison. Sedio and coworkers developed the chemical structural
141 compositional similarity (CSCS) metric²⁸ to account for relationships between molecules based
142 on the similarity of their fragmentation spectra. While CSCS compares samples based on
143 modified cosine scores obtained from molecular networking, we calculate chemical relationships
144 based on structurally-informed molecular fingerprints. We express these relationships in the form
145 of a hierarchy which enables the use of other tree-based tools for downstream data analyses. For
146 example, in Figure 2a, we show that by using a tree of structural relationships between molecules

147 in samples 1-3, we can apply UniFrac⁹, a tree-informed distance metric and demonstrate that the
 148 composition of sample 1 is distinct from samples 2 and 3.
 149

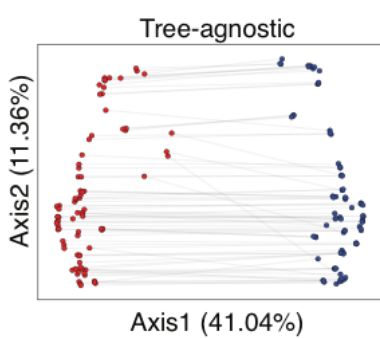
a.



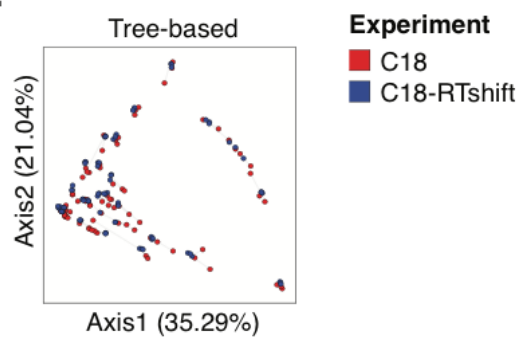
Do you account for
 molecular relatedness



b.



c.



150

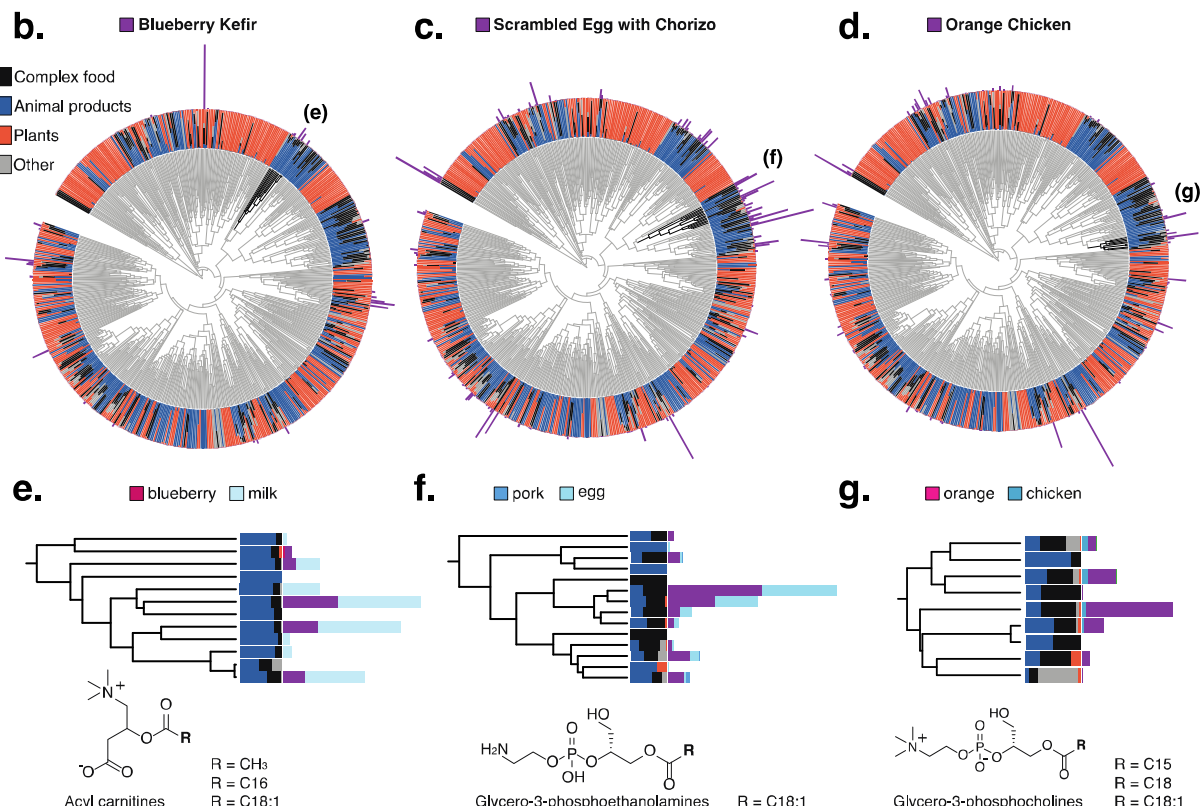
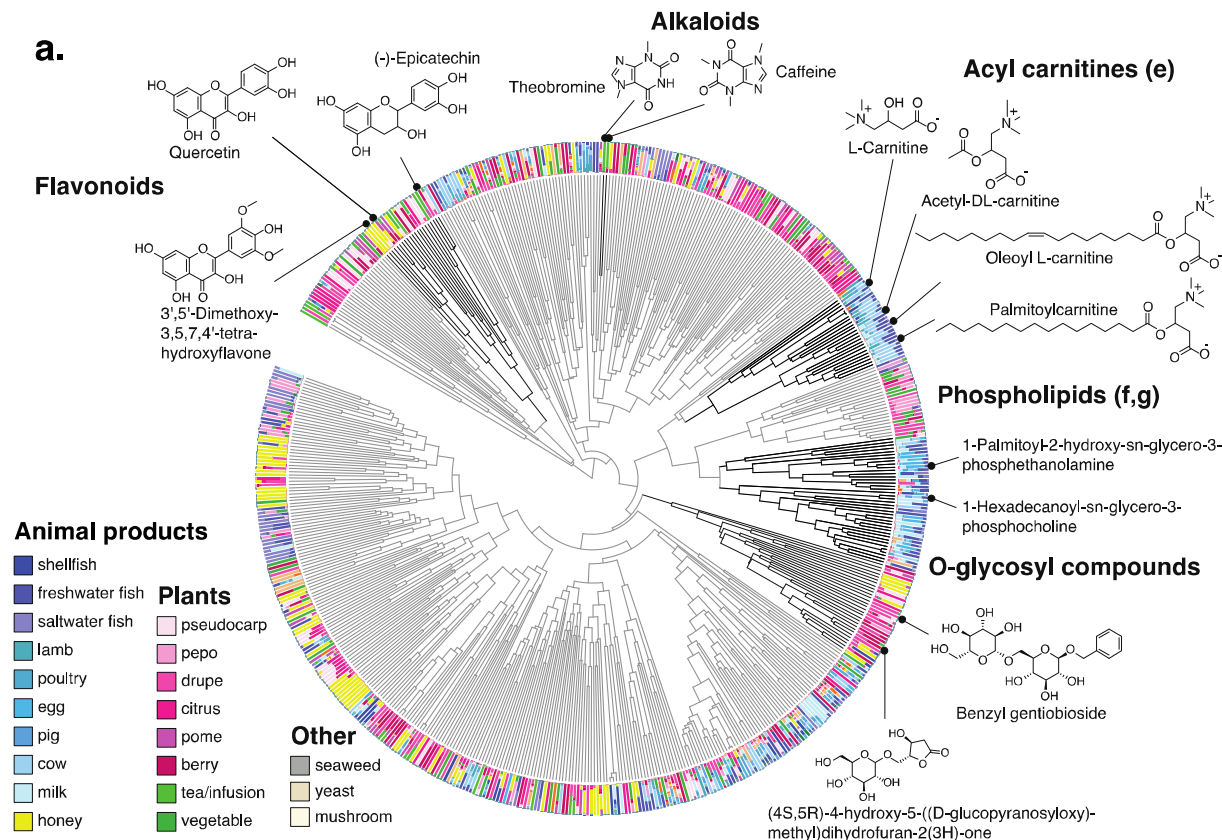
151 **Figure 2: The pitfalls of assuming equal relatedness of molecules and the advantages of a chemical tree for**
 152 **sample comparison. a)** A scenario where the goal is to compare the chemical composition in samples 1
 153 (sphingosine and phosphatidylcholine), 2 (glucose, galactose, and fructose), and 3 (sucrose and lactulose). When we
 154 do not account for the chemical relationships between the molecules, i.e. assume that the lipid molecules in sample 1
 155 are equally related to the sugars in samples 2 and 3 (left), we conclude that samples 1, 2, and 3 are similarly distinct.
 156 If we account for sugar molecules being more chemically related to one another than sugars are to lipid molecules

157 (right), we can obtain a chemically-meaningful distance between samples. This is exemplified through a principal
158 coordinates analysis (PCoA) of the computed UniFrac⁹ (tree-based) distances among samples; we see that samples 2
159 and 3 are more similar to each other, and sample 1 which is chemically distinct is separated along the primary axis
160 of variation, when distances are computed using the chemical tree. **b, c)** PCoA of samples in the evaluation dataset
161 colored by chromatography conditions. PCoA plot using tree-agnostic (Bray-Curtis²⁹) distances which do not
162 account for the chemical relationship between features detected across chromatography conditions (b) and tree-
163 based (Weighted UniFrac⁹) distances which are based on the hierarchical relationships between molecules in the
164 evaluation dataset (c).
165

166 The importance of comparing samples by accounting for their molecular relatedness is
167 highlighted when we contrast the results from ignoring the tree structure (Fig. 2b) to those which
168 integrate it (Fig. 2c). With the structural context provided by Qemistree, the differences between
169 replicates across batches are comparable to the within-batch differences (Fig. S2). The retention
170 time shift in this dataset leads to a strong technical signal that obscures the biological
171 relationships among the samples (permutational ANOVA; tree agnostic²⁹ pseudo-F=120.75,
172 p=0.001 vs. tree informed⁹ pseudo-F=18.2239, p=0.001). We observed and remediated a similar
173 pattern originating from plate-to-plate variation in a recently published study investigating the
174 metabolome and microbiome of captive cheetahs³⁰ (Fig. S3). In this study, placing the molecules
175 in a tree using Qemistree reduced the observed technical variation (Fig. S3 a, c), and highlighted
176 the dietary effect that was expected (Fig. S3 b, d). These results show how systematic and
177 spurious molecular differences can be mitigated in an unsupervised manner using chemically-
178 informed distance measures based on a tree structure.
179

180 As a case study, we used Qemistree to explore chemical diversity in a set of food samples
181 collected as a part of the Global FoodOmics initiative (<http://globalfoodomics.org>). We selected
182 a diverse range of food ingredients to represent animal, plant, and fungal groupings³¹. We first
183 performed feature-based molecular networking using MZmine^{17,18} to obtain spectral library
184 matches for a subset of the chemical features (~20% annotated with cosine cutoff > 0.7).
185 Understanding the chemical relationships between different foods is challenging because most
186 molecules within foods are unannotated. Using Qemistree, we collated GNPS spectral library
187 matches and *in silico* predictions from CSI:FingerID to annotate ~91% of the chemical features
188 (total 634 features after quality filtering) with molecular structures. Using ClassyFire²³, we
189 assigned a chemical taxonomy to 60% of these structures; the remaining 40% returned no
190 ClassyFire taxonomy. Labeling annotations allowed us to retrieve subtrees of distinct chemical
191 classes (Fig. 3a) such as flavonoids, alkaloids, phospholipids, acyl-carnitines, and O-glycosyl

192 compounds in food products. We propagated ClassyFire annotations of chemical features (tree
193 tips) to each internal node of the tree and labeled the nodes by pie charts depicting the
194 distribution in chemical superclasses (Fig. S4a) and classes (Fig. S4b) of its tips. The molecular
195 fingerprint-based hierarchy of chemical features agreed well with ClassyFire taxonomy
196 assignment, further demonstrating that molecular fingerprints can meaningfully capture
197 structural relationships among molecules in a hierarchical manner. Furthermore, Qemistree
198 coupled the chemical tree to sample metadata, revealing distinct chemical classes expected for
199 each sample type. Branches representing acyl-carnitines were exclusively found in animal
200 products (shades of blue; Fig. 3a). In contrast, honey, although categorized as an animal product,
201 shared most of its chemical space with plant products, reflective of the plant nectar and pollen-
202 based diet of honey bees. We observed a clade of flavonoids in both plant products and honey
203 (Figs. 3a, S4b), but no other animal-based foods.



205 **Figure 3: A chemical hierarchy of food-derived compounds based on predicted molecular fingerprints. a)** A
206 chemical tree based on molecular fingerprints representing the structural relationships between chemical features
207 (tree tips) detected in food products (single ingredient i.e. simple foods; N=119). The tree is pruned to only keep tips
208 that were assigned a structural annotation (SMILES) by either MS/MS spectral library match or *in silico* using
209 CSI:FingerID. All structures shown are spectral reference library matches obtained from feature-based molecular
210 networking in GNPS: (<https://gnps.ucsd.edu/ProteoSAFe/status.jsp?task=ceb28a199d6b4f4fbf08490d9c96d31>;
211 MSI level 3 annotation²⁷). The outer ring shows the relative abundance of each compound across a diverse range of
212 food sources (panel a legend; parsed at ‘sample_type_group4’ of the Global FoodOmics Project ontology). We
213 highlight clusters of compounds that are characteristic of specific food sources. For example, theobromine and
214 caffeine are two closely related xanthine compounds (top center); they are primarily seen in teas (light green
215 samples) and coffee beans (berry; purple). Similarly, acyl-carnitines and phospholipids (top right) are unique to
216 different animal products (blues). We note that honey (highlighted in yellow), although annotated as an animal
217 product, contains compounds that are primarily seen in plant sources (flavonoids, O-glycosyl compounds) and no
218 other animal products. Flavonoids (top left) are observed in a range of fruit, vegetable, and honey samples (but no
219 other animal products). **(b-d)** A hierarchy of the compounds observed in simple foods (above) and seven complex
220 samples: two meals of orange chicken, a cooked cucumber and the sauce from a meal (schmorgurken), sour cream,
221 blueberry kefir, and egg scramble with chorizo (N=126). The inner ring shows the relative abundance of each
222 compound across simple animal products, plant products, fungi and algae (other) and the 7 complex foods (black).
223 The absolute abundances of compounds in blueberry kefir (b), scrambled eggs with chorizo (c), and orange chicken
224 (d) (outer bars) are overlaid on the tree to illustrate the shared and unique chemistry of complex foods. A compound
225 subtree characteristic of each complex food in the tree is highlighted (black) and zoomed in **(e-g)**. **(e)** A subtree
226 showing the absolute abundance of acyl carnitines in blueberry kefir and its primary ingredients (blueberry and
227 milk). Similar subtrees showing phosphoethanolamine in scrambled eggs with chorizo (f), and phosphocholine in
228 orange chicken (g).
229

230 While it is expected that a complex food such as blueberry kefir contains molecules from both
231 blueberries and dairy, we can now visualize how individual ingredients and food preparation
232 contribute to the chemical composition of complex foods. We noted that metabolite signatures
233 that stem directly from particular ingredients, such as phosphoethanolamine from eggs, are
234 present in egg scramble (Fig. 3c), but not in the other two foods highlighted (Fig. 3b and d). We
235 can also observe the addition of ingredients in foods that were not listed as present in the initial
236 set of ingredients. We were able to retrieve that there is black pepper in the egg scramble with
237 chorizo and orange chicken, but that this signal is absent from the blueberry kefir (Fig. S5).
238

239 We show that our tree-based approach coherently captures chemical ontologies and relationships
240 among molecules and samples in various publicly available datasets. Qemistree depends on
241 representing chemical features as molecular fingerprints, and shares limitations with the
242 underlying fingerprint prediction tool CSI:FingerID. For example, fingerprint prediction depends
243 on the quality and coverage of MS/MS spectral databases available for training the predictive
244 models, and these will improve as databases are enriched with more compound classes.
245 Qemistree is also applicable in negative ionization mode; however, less molecular fingerprints

246 can be confidently predicted due to less publicly available reference spectra, resulting in less
247 extensive trees.

248

249 In summary, we introduce a new tree-based approach for computing and representing chemical
250 features detected in untargeted metabolomics studies. A hierarchy enables us to leverage existing
251 tree-based tools, and can be augmented with structural and environmental annotations, greatly
252 facilitating analysis and interpretation. We anticipate that Qemistree, as a data organization
253 strategy, will be broadly applicable across fields that perform global chemical analysis, from
254 medicine to environmental microbiology to food science, and well beyond the examples shown
255 here.

256

257 Data availability

258 The mass spectrometry data, metadata, and methods for the evaluation dataset have been
259 deposited on the GNPS/MassIVE public repository^{2,33} under the accession number
260 [MSV000083306](https://msv.gnps.ucsd.edu/MSV000083306). The parameters used for molecular networking are available on GNPS:
261 <https://gnps.ucsd.edu/ProteoSAFe/status.jsp?task=efda476c72724b29a91693a108fa5a9d>. The
262 chemical hierarchy generated by Qemistree (version 2020.1.2) is available on iTOL²⁴:
263 <https://itol.embl.de/tree/709513416494381587432576>.

264 The mass spectrometry data, metadata, and methods for Global Foodomics dataset have been
265 deposited on the GNPS/MassIVE public repository^{2,33} under the accession number
266 [MSV000085226](https://msv.gnps.ucsd.edu/MSV000085226). The parameters used for molecular networking are available on GNPS:
267 <https://gnps.ucsd.edu/ProteoSAFe/status.jsp?task=ceb28a199d6b4f4fb08490d9c96d631>. The
268 chemical hierarchy generated by Qemistree (version 2020.1.2) is available on iTOL²⁴:
269 <https://itol.embl.de/tree/13711034118313741584046018>.

270 Code availability

271 All source code is publicly available under BSD-2-Clause on GitHub:
272 <https://github.com/biocore/q2-qemistree>. Qemistree is also available as an advanced analysis
273 workflow on GNPS: <https://ccms-ucsd.github.io/GNPSDocumentation/qemistree/>
274

275 Acknowledgments

276 PCD was supported by the Gordon and Betty Moore Foundation (GBMF7622), the U.S. National
277 Institutes of Health for the Center (P41 GM103484, R03 CA211211, R01 GM107550), and the
278 University of Wisconsin-Madison OVCRG; LFN was supported by the U.S. National Institutes
279 of Health (R01 GM107550), and the European Union’s Horizon 2020 program (MSCA-GF,
280 704786). JJvdH was supported by an ASDI eScience grant, ASDI.2017.030, from the
281 Netherlands eScience Center—NLeSC. KD, MF, ML and SB were supported by Deutsche
282 Forschungsgemeinschaft (BO 1910/20).

283 Conflict of Interests

284 Mingxun Wang is a founder of Ometa Labs LLC.

285 Pieter C. Dorrestein is a scientific advisor for Sirenas LLC.
286 Kai Dührkop, Marcus Ludwig, Markus Fleischauer and Sebastian Böcker are founders of Bright
287 Giant GmbH.
288

289 References

290 1. Watrous, J. *et al.* Mass spectral molecular networking of living microbial colonies. *Proc.*
291 *Natl. Acad. Sci. U. S. A.* **109**, E1743–52 (2012).

292 2. Wang, M. *et al.* Sharing and community curation of mass spectrometry data with Global
293 Natural Products Social Molecular Networking. *Nat. Biotechnol.* **34**, 828–837 (2016).

294 3. Fox Ramos, A. E., Evanno, L., Poupon, E., Champy, P. & Beniddir, M. A. Natural products
295 targeting strategies involving molecular networking: different manners, one goal. *Nat. Prod.*
296 *Rep.* **36**, 960–980 (2019).

297 4. Böcker, S. & Dührkop, K. Fragmentation trees reloaded. *J. Cheminform.* **8**, 5 (2016).

298 5. Rasche, F. *et al.* Identifying the unknowns by aligning fragmentation trees. *Anal. Chem.* **84**,
299 3417–3426 (2012).

300 6. Washburne, A. D. *et al.* Phylogenetic factorization of compositional data yields lineage-
301 level associations in microbiome datasets. *PeerJ* **5**, e2969 (2017).

302 7. Faith, D. P. Conservation evaluation and phylogenetic diversity. *Biological Conservation*
303 vol. 61 1–10 (1992).

304 8. Janssen, S. *et al.* Phylogenetic Placement of Exact Amplicon Sequences Improves
305 Associations with Clinical Information. *mSystems* **3**, (2018).

306 9. McDonald, D. *et al.* Striped UniFrac: enabling microbiome analysis at unprecedented scale.
307 *Nat. Methods* **15**, 847–848 (2018).

308 10. Willett, P. Similarity-based virtual screening using 2D fingerprints. *Drug Discov. Today* **11**,

309 1046–1053 (2006).

310 11. Heinonen, M., Shen, H., Zamboni, N. & Rousu, J. Metabolite identification and molecular
311 fingerprint prediction through machine learning. *Bioinformatics* **28**, 2333–2341 (2012).

312 12. Laponogov, I., Sadawi, N., Galea, D., Mirnezami, R. & Veselkov, K. A. ChemDistiller: an
313 engine for metabolite annotation in mass spectrometry. *Bioinformatics* vol. 34 2096–2102
314 (2018).

315 13. Dührkop, K., Shen, H., Meusel, M., Rousu, J. & Böcker, S. Searching molecular structure
316 databases with tandem mass spectra using CSI:FingerID. *Proc. Natl. Acad. Sci. U. S. A.*
317 **112**, 12580–12585 (2015).

318 14. Fan, Z., Ghaffari, K., Alley, A. & Ressom, H. W. Metabolite Identification Using Artificial
319 Neural Network. *2019 IEEE International Conference on Bioinformatics and Biomedicine*
320 (*BIBM*) (2019) doi:10.1109/bibm47256.2019.8983190.

321 15. Li, Y., Kuhn, M., Gavin, A.-C. & Bork, P. Identification of metabolites from tandem mass
322 spectra with a machine learning approach utilizing structural features. *Bioinformatics* **36**,
323 1213–1218 (2020).

324 16. Dührkop, K. *et al.* SIRIUS 4: a rapid tool for turning tandem mass spectra into metabolite
325 structure information. *Nat. Methods* **16**, 299–302 (2019).

326 17. Pluskal, T., Castillo, S., Villar-Briones, A. & Oresic, M. MZmine 2: modular framework for
327 processing, visualizing, and analyzing mass spectrometry-based molecular profile data.
328 *BMC Bioinformatics* **11**, 395 (2010).

329 18. Nothias, L. F. *et al.* Feature-based Molecular Networking in the GNPS Analysis
330 Environment. *bioRxiv* 812404 (2019) doi:10.1101/812404.

331 19. Treutler, H. *et al.* Discovering Regulated Metabolite Families in Untargeted Metabolomics

332 Studies. *Anal. Chem.* **88**, 8082–8090 (2016).

333 20. Depke, T., Franke, R. & Brönstrup, M. Clustering of MS2 spectra using unsupervised
334 methods to aid the identification of secondary metabolites from *Pseudomonas aeruginosa*.
335 *Journal of Chromatography B* vol. 1071 19–28 (2017).

336 21. Rawlinson, C. *et al.* Hierarchical clustering of MS/MS spectra from the firefly metabolome
337 identifies new lucibufagin compounds. *Sci. Rep.* **10**, 6043 (2020).

338 22. Schymanski, E. L. *et al.* Critical Assessment of Small Molecule Identification 2016:
339 automated methods. *J. Cheminform.* **9**, 22 (2017).

340 23. Feunang, Y. D. *et al.* ClassyFire: automated chemical classification with a comprehensive,
341 computable taxonomy. *J. Cheminform.* **8**, 1–20 (2016).

342 24. Letunic, I. & Bork, P. Interactive Tree Of Life (iTOL) v4: recent updates and new
343 developments. *Nucleic Acids Res.* **47**, W256–W259 (2019).

344 25. Bolyen, E. *et al.* Reproducible, interactive, scalable and extensible microbiome data science
345 using QIIME 2. *Nat. Biotechnol.* **37**, 852–857 (2019).

346 26. Morton, J. T. *et al.* Learning representations of microbe-metabolite interactions. *Nat.*
347 *Methods* **16**, 1306–1314 (2019).

348 27. Sumner, L. W. *et al.* Proposed minimum reporting standards for chemical analysis.
349 *Metabolomics* vol. 3 211–221 (2007).

350 28. Sedio, B. E., Rojas Echeverri, J. C., Boya P., C. A. & Joseph Wright, S. Sources of
351 variation in foliar secondary chemistry in a tropical forest tree community. *Ecology* vol. 98
352 616–623 (2017).

353 29. Bray, J. R., Roger Bray, J. & Curtis, J. T. An Ordination of the Upland Forest Communities
354 of Southern Wisconsin. *Ecological Monographs* vol. 27 325–349 (1957).

355 30. Gauglitz, J. M. *et al.* Metabolome-informed microbiome analysis refines metadata
356 classifications and reveals unexpected medication transfer in captive cheetahs. *bioRxiv*
357 790063 (2019) doi:10.1101/790063.

358 31. Thompson, L. R. *et al.* A communal catalogue reveals Earth's multiscale microbial
359 diversity. *Nature* **551**, 457–463 (2017).

360 32. Morton, J. T. *et al.* Establishing microbial composition measurement standards with
361 reference frames. *Nat. Commun.* **10**, 2719 (2019).

362 33. Wang, M. *et al.* Assembling the Community-Scale Discoverable Human Proteome. *Cell*
363 *Syst* **7**, 412–421.e5 (2018).

364 34. Ludwig, M. *et al.* ZODIAC: database-independent molecular formula annotation using
365 Gibbs sampling reveals unknown small molecules. *bioRxiv* 842740 (2019)
366 doi:10.1101/842740.

367 35. Simón-Manso, Y. *et al.* Metabolite profiling of a NIST Standard Reference Material for
368 human plasma (SRM 1950): GC-MS, LC-MS, NMR, and clinical laboratory analyses,
369 libraries, and web-based resources. *Anal. Chem.* **85**, 11725–11731 (2013).

370 36. McDonald, D. *et al.* American Gut: an Open Platform for Citizen Science Microbiome
371 Research. *mSystems* **3**, (2018).

372 37. Martens, L. *et al.* mzML--a community standard for mass spectrometry data. *Mol. Cell.*
373 *Proteomics* **10**, R110.000133 (2011).

374 38. Chambers, M. C. *et al.* A cross-platform toolkit for mass spectrometry and proteomics. *Nat.*
375 *Biotechnol.* **30**, 918–920 (2012).

376